International Journal of Food Microbiology 382 (2022) 109930

Contents lists available at ScienceDirect

International Journal of Food Microbiology

journal homepage: www.elsevier.com/locate/ijfoodmicro

Transcriptomic and proteomic analysis of *Staphylococcus aureus* response to cuminaldehyde stress

Hui Li [a], Yan-yan Huang [b,c], Keren Agyekumwaa Addo [a], Ze-xuan Huang [a], Yi-gang Yu [a,*], Xing-long Xiao [a,*]

[a] Research Center of Food Safety and Detection, College of Food Science and Engineering, South China University of Technology, Guangzhou 510006, PR China
[b] College of Food Science and Engineering, Foshan University, Foshan 528225, PR China
[c] Guangdong Provincial Key Laboratory of Intelligent Food Manufacturing, Foshan University, Foshan 528225, PR China

ARTICLE INFO

Keywords:
Cuminaldehyde
Staphylococcus aureus
Antibacterial mechanism
Sauced beef
Transcriptomic
Proteomic

ABSTRACT

The previous study indicated that cuminaldehyde (CUM) could be used as an antibacterial agent in sauced beef to reduce the propagation of *Staphylococcus aureus* (*S. aureus*). This research took sauced beef treated with 0.4 μL/mL CUM as the research object. Transcriptomic and proteomic methods were used to comprehensively analyze the changes in genes and proteins of *S. aureus* under CUM stress. A total of 258 differentially expressed genes (DEGs, 178 up-regulated and 80 down-regulated) and 384 differentially expressed proteins (DEPs, 61 up-regulated and 323 down-regulated) were found. It was observed that CUM destroyed the cell wall and cell membrane by inhibiting the synthesis of peptidoglycan and fatty acid. Low energy consumption strategies were formed by reducing glycolysis and ribosome de novo synthesis. The levels of genes and proteins associated with the glycine, serine, threonine, methionine, cysteine, and branched-chain amino acids were dramatically changed, which impaired protein synthesis and reduced bacterial viability. In addition, the up-regulated DEGs and DEFs involved in DNA replication, recombination and single-stranded DNA-binding contributed to DNA repair. Moreover, ATP-binding cassettes (ABC) transporters were also perturbed, such as the uptake of betaine and iron were inhibited. Thus, this study revealed the response mechanism of *S. aureus* under the stress of CUM, and provided a theoretical basis for the application of CUM in meat products.

1. Introduction

Staphylococcus aureus, a gram-positive bacterium, is not only one of the most prominent human pathogens, but also one of the main food-borne and iatrogenic pathogens related to various diseases (Ghosh et al., 2016). This may be due to easy transmission, high carrying rate, and cross-protective stress response system of *S. aureus* (Dupre et al., 2019). Foods of animal origin rich in protein, including meat and processed meat, are often involved in staphylococcal infection (Hennekinne et al., 2012). According to the report on the *S. aureus* outbreak in the United States from 1998 to 2008, meat and poultry dishes were the most common food sources, of which the outbreak rate of *S. aureus* accounted for 55 % (Bennett et al., 2013). The causes of the outbreaks were related to improper storage temperature, incomplete sterilization, infection of food handlers, and environmental pollution (European Food Safety et al., 2017). In addition, *S. aureus* has proteases that degrade external protein sources, a variety of amino acids, and oligopeptide transporters, allowing it to multiply rapidly on meat (Dubin, 2002). *S. aureus* can also decompose >10 amino acids to produce necessary metabolic intermediates (Halsey et al., 2017). Therefore, much attention should be considered to the risk of *S. aureus* infection in meat products.

Food preservatives are often used in the food processing industry to reduce the propagation of microorganisms (Wei et al., 2019). However, many synthetic additives have been misused to prolong the shelf life of food over the years, resulting in negative impacts on residual toxicity and teratogenicity (Das et al., 2021). Thus, it requires the necessity to find safe and efficient natural preservatives to maintain food quality. Cuminaldehyde (CUM), *p*-Isopropylbenzaldehyde, is the main component of cumin essential oil. It is considered safe and widely applied in food and spices. It is also an essential raw material and intermediate in synthesizing high-grade spices and other organic chemical products. CUM exhibits bioactive properties, such as anti-fungus, antibacterial and

* Corresponding authors at: Research Center of Food Safety and Detection, College of Food Sciences and Engineering, South China University of Technology, 381Wushan Road, Tianhe District, Guangzhou City, Guangdong Province 510640, PR China.
E-mail addresses: yuyigang@scut.edu.cn (Y.-g. Yu), fexxl@scut.edu.cn (X.-l. Xiao).

https://doi.org/10.1016/j.ijfoodmicro.2022.109930
Received 13 May 2022; Received in revised form 4 September 2022; Accepted 9 September 2022
Available online 13 September 2022

antioxidant (Xu et al., 2021). In addition, it has an antibacterial effect on a variety of pathogens such as *Escherichia coli* (*E. coli*), *Listeria monocytogenes* (*L. monocytogenes*), and *Salmonella* spp. (Monteiro-Neto et al., 2020). Previous work revealed that CUM could damage the *S. aureus* cell membrane and further interact with DNA, thereby interfering with gene expression and protein synthesis, resulting in cell inactivation (Li et al., 2022b). And it also could reduce the production of exotoxins (hemolysin, enterotoxin, etc) by regulating the gene *sarA*, and directly bind to Tyrosine 149 and Proline 151 of monomeric α-hemolysin to inhibit the formation of heptamers, thereby decreasing hemolysin activity (Li et al., 2022a). However, there is still no comprehensive understanding and clarification of the control mechanism of CUM on pathogens in food substrates.

Therefore, the alteration of differentially expressed genes (DEGs) and differentially expressed proteins (DEPs) of *S. aureus* after CUM treatment were analyzed by the combination of transcriptomic and proteomic data. Afterward, the Gene Ontology (GO) category and Kyoto encyclopedia of genes and genomes (KEGG) pathway enrichment analysis were conducted to shed light on the potential action of CUM on *S. aureus*.

2. Materials and methods

2.1. Reagents and strain

S. aureus (ATCC 29213) was obtained from Shanghai Luwei Technology Co., Ltd. (Shanghai, China). A colony was cultured in a tryptic soy broth (TSB; Huankai Microbial Technology Co., Ltd., Guangzhou, China) medium at 37 °C for 24 h. CUM (≥97 %) was obtained from Shanghai Aladdin Biochemical Co., Ltd. (Aladdin, Shanghai, China).

2.2. Survival rate of S. aureus treated with CUM in sauced beef

Samples were prepared with reference to the previous article (Li et al., 2022a). The beef with spices was simmered for 2 h, cut into 1.5 g and sterilized at 121 °C for 15 min to obtain sauced beef samples (1.0 g) with a mass loss of about 0.5 g. After cooling to room temperature, the samples were inoculated with *S. aureus*. After 30 min, these inoculated samples were treated with or without 0.4 μL/mL CUM for 5 min, and then kept in a thermostatic incubator under 37 °C for 10 h. Afterward, the number of *S. aureus* was measured using the pour-plating method every 2 h. The sauced beef (10.0 g) was mixed with 90 mL of sterile saline solution (0.85 %, m/v). The diluted bacterial solution was cultured in mannitol salt agar (Huankai Microbial Technology Co., Ltd., Guangzhou, China) at 37 °C for 24 h.

2.3. S. aureus stressed by CUM

Sauced beef samples were treated by following the steps described above, and then cultured for 6 h. *S. aureus* attached to sauced beef was swirled into sterile water, and the minced meat in the bacteria solution was removed by filtration with sterile gauze (500 mesh). The bacterial precipitation was obtained by centrifuging at 8000 ×*g* for 3 min, and then was frozen rapidly in liquid nitrogen. The *S. aureus* cells collected from the treatment and control groups were divided into two groups. One group was used to extract RNA and the other group was used to extract protein.

2.4. Transcriptomic analysis of S. aureus stressed by CUM

2.4.1. RNA extraction and Illumina sequencing

Total RNA was isolated from samples using TRIzol reagent. RNA degradation degree and potential contamination were detected with agarose gels. RNA purity and integrity were examined using the NanoPhotometer® spectrophotometer (IMPLEN, CA, USA) and Bioanalyzer 2100 (Agilent, Santa Clara, CA). The rRNA was removed by Illumina MRZB12424 Ribo-Zero rRNA Removal Kit (Illumina, San Diego, CA, USA). As mentioned in the previous paper (Cao et al., 2020), the construction of the cDNA library was completed.

2.4.2. Transcriptomic data analysis

The original data was screened by discarding low-quality readings, including 10 % unknown nucleotides and >50 % bases. Gene expression levels were established using Reads Per Kilobase per Million (FPKM) mapped reads method. Edger software was used to calculate the DEGs based on the combined criteria of fold change >2 and a false discovery rate-adjusted $p < 0.05$. Then, DEGs were enriched by GO function and KEGG pathways, and $p < 0.05$ was considered as the threshold.

2.5. Proteomic analysis of S. aureus stressed by CUM

2.5.1. Protein extraction, quantification, digestion and nano-HPLC-MS/MS analysis

The protein was isolated from the sample and the protein concentration was measured by BCA Protein Assay Kit. DTT and iodoacetamide were used to break the disulfide bond and reductive alkylation of the protein to hydrolyze the protein fully. The proteins were then digested with Trypsin. Online nanospray LC-MS/MS on an Orbitrap Fusion™ Lumos™ coupled to EASY-nLC 1200 system (Thermo Fisher Scientific, MA, USA) was used for analysis, and the data acquisition mode was data dependent acquisition (DDA).

2.5.2. Proteomic data analysis

PEAKS Studio version X (Bioinformatics Solutions Inc., Waterloo, Canada) mass spectrometry was used for analysis. When differences in protein expression between the CUM and the control groups were >1.2-fold change, with $p < 0.05$, the protein was considered DEPs. The GO enrichment method was used to classify the GO annotated proteome. GO with $p < 0.05$ after the correction was deemed to be significant. The enrichment of DEPs in the KEGG pathway was detected by KAAS software. KEGG enrichment analysis was helpful to further analyze the biological functions of DEPs.

2.6. Quantitative reverse transcriptional PCR (qRT-PCR) validations

The DEGs were randomly selected for qRT-PCR analysis to validate the results of RNA-sequencing (RNA-seq). Total RNA was isolated from the cells of *S. aureus* using TRIzol reagent. The isolated RNA was reverse-transcribed to cDNA using Robust First Strand cDNA Synthesis Kit (Yingzan, Guangzhou, China). Subsequently, qRT-PCR reactions were carried out to evaluate the transcription levels in Table 1 using the SYBR Green method, and the *16 s rRNA* was used as an internal standard to normalize the expression levels.

3. Results

3.1. Survival rate of S. aureus treated with CUM in sauced beef

Changes in the numbers of *S. aureus* cells cultured in sauced beef with

Table 1
Genes and the corresponding primers used for qRT-PCR analysis.

Gene	Nucleotide sequence of primers (5′-3′)	
	Forward primer	Reverse primer
sea	ATGGTGCTTATTATGGTTATC	CGTTTCCAAAGGTACTGTATT
hly	AACCAGATGTTCTCCCTGAT	CACTGTAAGCCATTTCGTCA
agrA	TGATAATCCTTATGAGGTGCTT	CACTGTGACTCGTAACGAAAA
sarA	TCTTGTTAATGCACAACAACGTAA	TGTTTGCTTCAGTGATTCGTTT
luxS	CATACCCTGGAGCACCTGTT	TGATCCTGCACTTTCAGCAC
ilvD	TGTCACAGTTTGGGATGTAGAA	CCTTCCCTCTCGTGAAGTTATC
16S rRNA	GCTGCCCTTTGTATTGTC	AGATGTTGGGTTAAGTCCC

or without CUM treatment were shown in Fig. 1. Approximately 1 log CFU/g of reduction was found under CUM treatment for 6 h compared to the control. It could be seen that CUM displayed an inhibitory impact on the growth of *S. aureus*. In addition, the study found that the most appropriate treatments for transcriptome analysis were stress response conditions for high cell survival rate and a large number of sublethal cells (Chueca et al., 2017). Therefore, *S. aureus* treated with 0.4 μL/mL of CUM in sauced beef for 6 h was selected to obtain valuable transcriptomic and proteomic data. *S. aureus* without exposure to CUM was used as the control (CK). It is worth mentioning that the researchers cultured L. *monocytogenes* in ready to eat (RTE) meat, but failed to extract total RNA from the cells cultured in RTE meat to meet the quality requirements of RNA-seq analysis, and finally studied the action mechanism of sodium lactate on L. *monocytogenes* in the culture medium (Suo et al., 2018). In the previous study of the research group, the antibacterial mechanism of thymol and cinnamaldehyde on L. *monocytogenes* in autoclaved chicken breast was discussed through transcriptome (Liang et al., 2022). This might be related to multiple extraction and enrichment method adopted by the research group in extracting RNA from the food matrix, that was, the enrichment of RNA from multiple extractions was conducive to obtaining enough RNA. Moreover, it was of tremendous theoretical value to apply CUM in meat rather than the culture medium to study the antibacterial mechanism.

3.2. Transcriptomic analysis for S. aureus under CUM stress

The influence of CUM stress on *S. aureus* transcriptome was determined by RNA-seq. The relative gene expression levels were calculated by comparing CUM-treated *S. aureus* with non-treated *S. aureus*. After data filtering, a total of 258 DEGs were screened in the CUM group, of which 178 were up-regulated and 80 were down-regulated compared with the control group (Fig. 2 and Table S1).

To further understand the functional categories of the DEGs under CUM treatment, DEGs were divided into 44 functional sub-categories. Fig. S1a showed that the GO system has three ontologies: biological process, cellular component and molecular function. The DEGs were centrally distributed in the terms “cellular process”, “single-organism process”, and “metabolic process” in biological process. GO terms, which were rich in cellular components, referred to “cell part”, “cell” and “membrane”. In terms of molecular function, most DEGs were distributed in “catalytic activity”, “binding” and “transporter activity”.

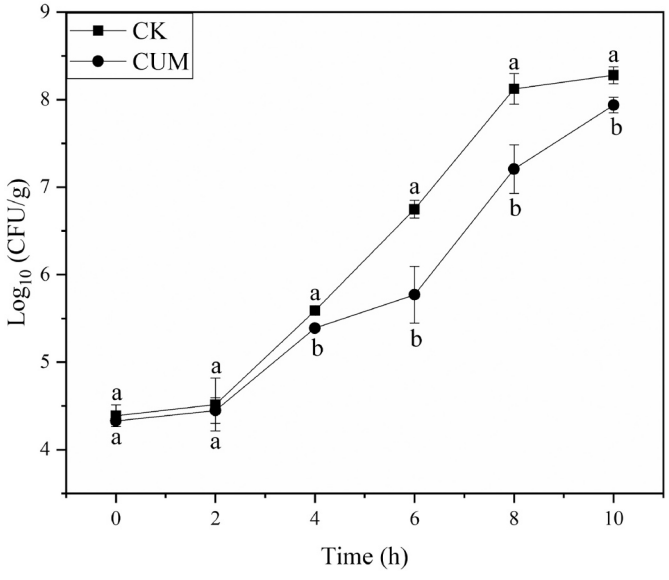

Fig. 1. The growth status of *S. aureus* when coping with/without cuminaldehyde (CUM) in sauced beef at 37 °C.

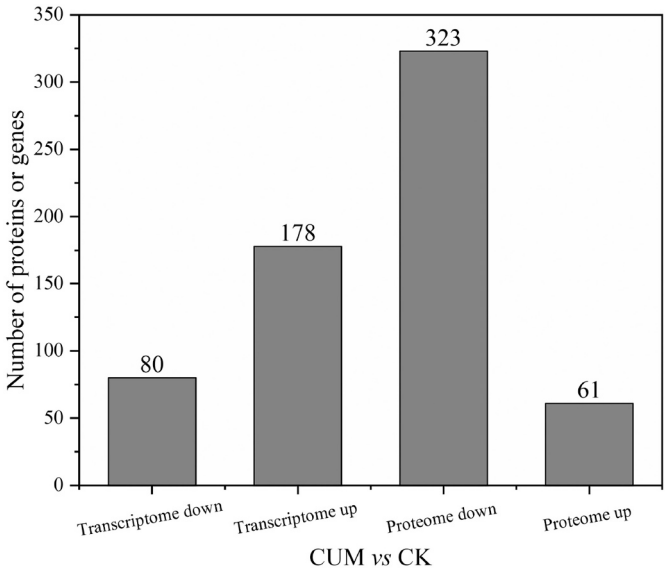

Fig. 2. The profile of differentially expressed genes (DEGs) and differentially expressed proteins (DEPs) of *S. aureus* exposed to cuminaldehyde (CUM) group compared with control group.

In addition, KEGG pathway enrichment analysis demonstrated that DEGs were primarily associated with biosynthesis of secondary metabolites, biosynthesis of amino acids, 2-Oxocarboxylic acid metabolism, valine, leucine and isoleucine biosynthesis (Fig. S2a).

3.3. Proteomic analysis for S. aureus under CUM stress

The responses of *S. aureus* to CUM stress at the protein level were evaluated by the label-free-based method. A total of 9631 peptides and 1318 proteins were found in *S. aureus* in this study (Fig. S3a). Most of the identified peptide sequences were in the range of 8 to 13 (Fig. S3b). The coverage of different peptide sequences was shown in Fig. S3c. Among them, 667 proteins covered <30 %, accounting for 50.61 % of all identified proteins. There were 449 proteins covering 30–60 %, accounting for 34.06 %. There were 202 proteins covering >60 %, accounting for 15.32 % of all identified proteins. After data filtering, 384 DEPs were observed compared with the control group after CUM treatment, of which 61 were up-regulated and 323 were down-regulated (Fig. 2 and Table S2).

The enriched GO functional groups were determined by GO analysis. DEPs were classified according to biological process, cellular component and molecular function, and then they were annotated and divided into different functional groups (Fig. S1b). After treatment with CUM, GO was enriched by biological processes including “cellular process”, “metabolic process”, and “single-organism process”. For cellular components, the enriched components mainly had “cell”, “cell part” and “macromolecular complex”, while for molecular functions, the central enrichments were “binding” and “catalytic”. Furthermore, KEGG analysis demonstrated that DEPs mainly were enriched in a metabolic pathway, biosynthesis of amino acids, and carbon metabolism (Fig. S2b).

3.4. The correlation analysis of DEGs and DEPs

The correlation between the transcriptomic and proteomic data was analyzed. By comparing identified 2453 genes and 1318 proteins, 754 proteins with their encoding genes were found at transcript and protein levels (Fig. 3a and Table S3). The correlation between DEGs and DEPs was shown in Fig. 3a, b, and c, indicating that the expression of genes and proteins does not always match. In addition, the regulation of some

DEGs and DEPs showed the opposite trend (TDPU and TUPD in Fig. 3b).

A single method cannot adequately explain the complexity of basic biology (Nie et al., 2007). Nevertheless, as reported in other research, the low correlation between mRNAs and proteins abundance was a question in research by transcriptomic and proteomic analyses (Lv et al., 2017; An et al., 2014). In the experiment, 2453 genes were found by transcriptome analysis, but most of the protein products of these genes were not found by proteome analysis. Many variables affect the correspondence between mRNA level and protein abundance from transcription to translation. The mRNA was translated into protein, but transcription and translation were not necessarily related. All regulatory processes in cells such as protein synthesis, processing, and modification were not reflected by transcriptome data (Vogel and Marcotte, 2012). The correlation between transcriptomics and proteomics was usually modest, and protein abundance could not always be predicted by mRNA levels (Gao et al., 2020). In addition, some proteins could be transported from intracellular to extracellular or degraded instantly, and proteins with low abundance could not be detected by proteomics (Kumar et al., 2016). Although the expression of some genes and proteins were not directly related, these changes were complementary, which was conducive to a comprehensive understanding of *S. aureus* against CUM stress.

3.5. qRT-PCR validation

Six genes were selected for qRT-PCR analysis, of which one gene was up-regulated and five genes were down-regulated, which was used to verify the transcriptomic and proteomic data of previous experiments (Table 2). It could be seen from Fig. 4 that qRT-PCR data has a good correlation with RNA-seq ($R^2 = 0.8977$). In general, the results of transcriptomics and proteomics were reliable.

4. Discussion

The responses of *S. aureus* to CUM stress were quite complex procedures associated with different pathways (Table 2). Full details were discussed below, and the proposed mechanism model of regulatory pathways was established in Fig. 5.

4.1. Cell envelope damage

The cell envelope is the pivotal protective shield to fight adverse environments (Zhao et al., 2022). Peptidoglycan and teichoic acid are the principal components of the cell wall of Gram-positive bacteria. After CUM stress, the abundance of three proteins, UDP-*N*-acetylglucosamine 1-carboxyvinyltransferase (MurA), UDP-*N*-acetylenolpyruvoylglucosamine reductase (MurB), UDP-*N*-acetylmuramoyl-tripeptide-$_D$-alanyl-$_D$-alanine ligase (MurF) involved in the peptidoglycan biosynthesis, were obviously decreased (Table 2). MurA can add enolpyruvyl to UDP-*N*-acetylglucosamine to catalyze the biosynthesis of peptidoglycans (Alhaji Isa et al., 2018). MurB catalyzes the final step in forming UDP-*N*-acetylteichoic acid (UDP-MurNAc), which can act as an essential catalyst in the presence of NADPH to catalyze enolpyruvyl UDP-*N*-acetylglucosamine to UDP-MurNAc (Amera et al., 2020). The final step in synthesizing peptidoglycan is the production of the UDP-MurNAc-pentapeptide by MurF enzyme (Poopandi et al., 2021). In addition, tandem lipoprotein involved in forming long glycan chains was dramatically down-regulated by 1.25 log2(FC) both at transcript and protein levels in CUM-treated *S. aureus*. It was worth mentioning that monomycin antibiotics could combine with glycosyltransferases to exert antibacterial effects, and this antibiotic has been used for decades without resistance (Ostash and Walker, 2010). Glycosyltransferase was obviously down-regulated at the protein level, indicating that CUM targeting glycosyl transferase had a vital application value. Meanwhile,

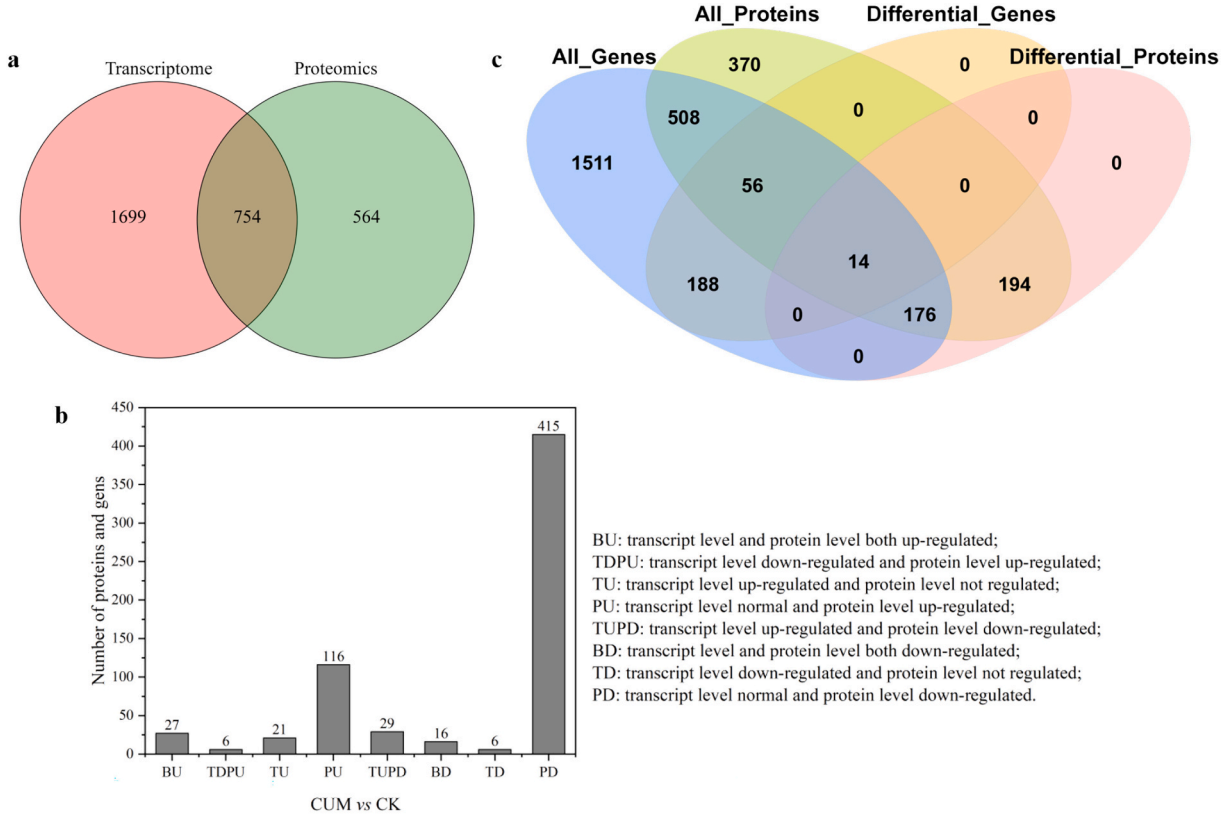

Fig. 3. The correlation between identified genes and proteins of *S. aureus* in response to cuminaldehyde (CUM) stress. (A) Comparison of the number of identified transcripts and proteins. (B) The classification of differentially expressed genes (DEGs) and differentially expressed proteins (DEPs). (C) Venn diagram of DEGs and DEPs in CUM *vs.* control group.

Table 2
Differentially expressed genes (DEGs) and differentially expressed proteins (DEPs) in *S. aureus* exposed to CUM stress.

Gene ID	Gene	Protein ID	Fold change Log2(FC)		Description
			Transcriptomic	Proteomic	
Cell surface					
BJI72_RS10790	*murA2*	WP_000046602.1	0.15	−1.04	UDP-*N*-acetylglucosamine 1-carboxyvinyltransferase
BJI72_RS03845	*murB*	WP_000608433.1	−0.06	−0.99	UDP-*N*-acetylenolpyruvoylglucosamine reductase
BJI72_RS10565	*murF*	WP_000611464.1	−0.06	−0.77	UDP-*N*-acetylmuramoyl-tripeptide–$_{D}$-alanyl-$_{D}$-alanine ligase
BJI72_RS02360	*lpl9*	WP_001802016.1	−1.25	−1.25	Tandem lipoprotein, partial
BJI72_RS06955	*ponA*	WP_000138351.1	−0.32	−0.70	Glycosyl transferase
BJI72_RS05900	*sepF*	WP_017431819.1	−0.64	−0.83	Cell division protein SepF
BJI72_RS05315	*ktrC*	WP_000514290.1	−0.57	−1.07	TrkA potassium uptake family protein
BJI72_RS07815	*accC1*	WP_000942744.1	−0.84	−1.33	Acetyl-CoA carboxylase biotin carboxylase subunit
BJI72_RS06125	*acpP*	WP_000426914.1	1.06	2.49	Acyl carrier protein
BJI72_RS07820	*BCCP1*	WP_001019340.1	−0.78	−0.71	Biotin carboxyl carrier protein
Energy metabolism					
BJI72_RS07485	*glkA*	WP_000161314.1	0.30	−0.23	Glucokinase
BJI72_RS04655	*pgi*	WP_000148852.1	−0.12	−2.61	Glucose-6-phosphate isomerase
BJI72_RS13980	*manP*	WP_000706111.1	0.55	0	PTS transporter subunit EIIA
BJI72_RS00510	*SAUSA300_0194*	WP_000159750.1	−0.10	−2.83	PTS transporter subunit EIIC
BJI72_RS06730	*odhA*	WP_000180673.1	−0.59	0.84	2-oxoglutarate dehydrogenase E1 component
BJI72_RS05355	*pdhB*	WP_000068176.1	0.18	−0.65	Pyruvate dehydrogenase complex, E1 component subunit beta
BJI72_RS01365	*SAV0354*	WP_000199067.1	−0.01	−0.81	Acetyl-CoA acetyltransferase
BJI72_RS08305	*ytsJ*	WP_000058389.1	0.06	−0.23	Malate dehydrogenase (oxaloacetate-decarboxylating), partial
BJI72_RS08275	*citZ*	WP_000829167.1	−0.16	−0.01	Isocitrate dehydrogenase
BJI72_RS04540	*SA0802*	WP_000046076.1	−0.34	−0.86	NADH dehydrogenase-like protein SAUSA300_0844
BJI72_RS10700	*atpF*	WP_000140679.1	−0.14	−2.01	F0F1 ATP synthase subunit B
BJI72_RS10685	*atpG*	WP_000157603.1	−0.40	1.36	F0F1 ATP synthase subunit gamma
BJI72_RS10675	*atpC*	WP_001094394.1	−0.22	−0.62	F0F1 ATP synthase subunit epsilon
BJI72_RS10695	*atpH*	WP_000241344.1	−0.03	−0.28	ATP synthase subunit delta
BJI72_RS05305	*ythA*	WP_000381849.1	−0.20	−2.30	Cytochrome *d* ubiquinol oxidase subunit I
Amino acids biosynthesis and metabolism					
BJI72_RS02815	*SAV0550*	WP_000250823.1	−0.16	−0.67	2-amino-3-ketobutyrate CoA ligase
BJI72_RS01205	*SAV0324*	WP_000731878.1	−0.10	−0.36	Glycine cleavage system H-like protein
BJI72_RS10730	*glyA*	WP_000120494.1	−0.12	−0.74	Serine hydroxymethyltransferase
BJI72_RS02070	*mccB*	WP_001036648.1	−1.15	1.91	Cys/Met metabolism PLP-dependent enzyme
BJI72_RS13500	*mtnE*	WP_000625061.1	0.26	−1.67	Transaminase
BJI72_RS02835	*ilvE*	WP_000076036.1	0.16	−0.66	Branched-chain amino acid aminotransferase
BJI72_RS10405	*leuA*	WP_000094583.1	−1.62	−2.52	2-isopropylmalate synthase
BJI72_RS07335	*bfmBAA*	WP_000568351.1	−0.48	−1.40	Branched-chain alpha-keto acid dehydrogenase E1 component
Ribosome					
BJI72_RS02485	*rplY*	WP_000157650.1	−1.13	−0.34	50S ribosomal protein L25/general stress protein Ctc
BJI72_RS07640	*rsmE*	WP_001190120.1	1.46	−2.68	Ribosomal RNA small subunit methyltransferase E
BJI72_RS04940	*prfC*	WP_001049950.1	0.39	−0.50	Peptide chain release factor 3 (RF-3)
BJI72_RS08095	*folC*	WP_001108346.1	−0.09	−0.82	Dihydrofolate synthase
DNA repair					
BJI72_RS09430	*dnaC*	WP_031769012.1	3.65	2.57	DNA replication protein DnaC
BJI72_RS06970	*dnaD*	WP_000362218.1	0.38	1.00	DNA replication protein DnaD
BJI72_RS05635	*mutS2*	WP_001249272.1	0.06	2.92	Recombination and DNA strand exchange inhibitor protein
BJI72_RS09455	–	WP_000840496.1	2.98	1.71	Single-stranded DNA-binding protein
BJI72_RS12925	–	WP_000759682.1	0.38	−1.86	DNA polymerase III alpha subunit
ABC transporters					
BJI72_RS04770	*oppB*	WP_000521533.1	1.35	−2.11	Oligopeptide ABC transporter, permease protein
BJI72_RS04780	*oppD*	WP_000140050.1	0.36	1.67	Oligopeptide ABC transporter, ATP-binding protein
BJI72_RS04785	*oppF*	WP_000786734.1	0.39	0.81	Oligopeptide ABC transporter ATP-binding protein
BJI72_RS07525	*fur*	WP_001095260.1	−0.47	−0.34	ABC transporter permease protein
BJI72_RS04775	*dppC*	WP_000829632.1	0.68	−0.67	ABC transporter permease
BJI72_RS12105	*hrtB*	WP_031769106.1	0.92	−0.73	ABC transporter, permease
BJI72_RS12615	*opuCC*	WP_000721551.1	−0.68	−1.17	Substrate-binding region of ABC-type glycine betaine transport system
BJI72_RS03315	*fhuC*	WP_001080809.1	−0.58	−0.22	Iron compound ABC transporter ATP-binding protein
BJI72_RS03295	*bmrA*	WP_031769037.1	−0.29	−2.79	ABC transporter, ATP-binding protein
BJI72_RS01125	*lolD*	WP_031769063.1	−0.18	0.29	ABC transporter, ATP-binding protein
BJI72_RS00740	*nikA*	WP_000669656.1	0.24	−2.19	ABC transporter, substrate-binding protein
BJI72_RS11100	*yfmC*	BJI72_RS11100	0.31	−1.54	ABC transporter substrate-binding protein
BJI72_RS12670	*fetA*	WP_000923526.1	0.38	−0.47	ABC transporter related
BJI72_RS11995	*yhaQ*	WP_000524830.1	0.11	−0.33	ABC transporter related
BJI72_RS09205	*ecsA*	WP_000216874.1	0.45	−1.27	ABC transporter related
BJI72_RS09585	*metN2*	WP_000571213.1	0.72	−1.90	ABC transporter related

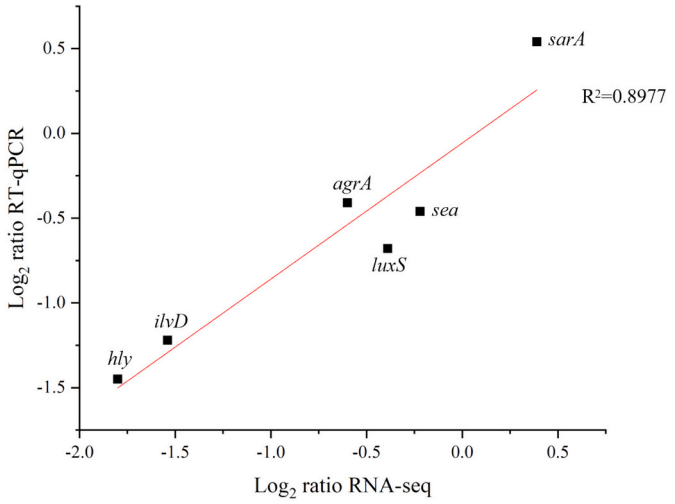

Fig. 4. qRT-PCR validation.

sepF encoding cell division protein, and *ktrC* encoding TrkA potassium uptake family protein, were all down-regulated both at transcript and protein levels in this study. A previous study showed that the cell division of *E. coli* involved a series of essential proteins, which were assembled in the middle of the cell to form so-called mitosomes. It regulated intimal invagination, cell wall synthesis, and outer membrane inward growth. TrkA is a homologue of a potassium absorbing protein that is thought to be necessary for homeostasis in response to environmental changes. The above results showed that CUM had a specific damage effect on the cell wall of *S. aureus*, mainly by inhibiting the synthesis of peptidoglycan, the main component of the cell wall.

As the hydrophobic end of phospholipids and lipopolysaccharides, fatty acids play a critical role in cell membrane permeability. The permeability and integrity of the cytoplasmic membrane are significant for maintaining bacteria's normal physiological processes and cell viability. In the previous study, the antibacterial activity of CUM was mainly due to its undue influence on cell membrane integrity and permeability (Li et al., 2022b). Acetyl-CoA carboxylase (ACC) and acyl carrier protein (ACP) are the first steps in the irreversible catalysis of fatty acid biosynthesis. ACP was overexpressed both at transcript and protein levels after CUM stress. Probably related to the need for enhanced lipid biosynthesis, which could restore the damaged membrane on the one hand and improve the survival of cells with sublethal damage on the other hand. However, *accC* encoding the biotin carboxylase subunit of ACC, which catalyzes the committed step in long chain fatty acid synthesis, and *BCCP* encoding biotin carboxyl carrier protein, which catalyzes the carboxylation of acetyl-CoA to malonyl-CoA, were all down-regulated both at transcript and protein levels (Table 2). Therefore, these findings manifested that the synthesis of fatty acids was inhibited after CUM treatment and thus destroyed the membrane's permeability.

4.2. Energy metabolism

Glycolysis, tricarboxylic acid cycle (TCA cycle) and electron transport chain (ETC) are necessary energy supply processes for heterotrophic cells. The energy supply system of *S. aureus* was changed under CUM stress. The protein abundance of PTS transporter subunit EIIC in the phosphotransferase system (PTS) was reduced significantly, with the encoding gene not differentially expressed (Table 2). PTS can transfer extracellular saccharides to the cell membrane and phosphorylate them. Therefore, PTS is considered a fuel source for the glycolytic pathway (Cao et al., 2011). Meanwhile, the reaction catalyzed by glucokinase was an energy-consuming process, and the decrease in its protein abundance suggested that *S. aureus* might conserve energy by inhibiting glycolysis (Zhao et al., 2022). Glucose-6-phosphate isomerase reversibly converts glucose 6-phosphate to fructose 6-phosphate, a process essential for upstream glycolysis and gluconeogenesis. However, glucose 6-phosphate isomerase was obviously decreased at the protein level. In sum, the conversion of glucose to phosphoenolpyruvate was inhibited during glycolysis.

Acetyl-CoA is the core part of energy metabolism and can interact with various anabolic pathways. After CUM treatment, the protein levels of acetyl-CoA production-related proteins, encoding acetyl-CoA acetyltransferase (AtoB) and pyruvate dehydrogenase, were decreased evidently. Other DEPs, malate dehydrogenase (MDH) and isocitrate dehydrogenase (ICDH) associated with the TCA cycle were also slightly down-regulated after CUM treatment. MDH is an important enzyme in the TCA cycle, which significantly impacts the TCA cycle. For example, the active part of poplar bud essential oil mainly restrained the TCA cycle by decreasing the activity of MDH (Yang et al., 2016), which was consistent with the results of this study. ICDH oxidizes isocitrate to form α-ketoglutaric acid. A previous study found that citral reduced the ICDH activity in *Penicillium digitatum*, which eventually led to the disorder of the TCA cycle (Zheng et al., 2015). Moreover, the expression of *odhA* was down-regulated at the mRNA level but significantly up-regulated at the protein level. Gene, *odhA* encodes a component of 2-oxoglutarate dehydrogenase complex that catalyzes the formation of 2-oxoglutarate to succinyl-CoA and then further forms succinate through succinyl-CoA transferase. These regulated genes and proteins stated that the TCA cycle in *S. aureus* was disrupted.

Notably, the NADH and $FADH_2$ generated during the TCA cycle are involved in oxidative phosphorylation via ETC, ultimately generating energy. The obvious down-regulation of dehydrogenase at the protein level restrained the synthesis of NADH, which was involved in the electron transport pathway intimately related to the TCA cycle, producing ATP for energy metabolism. In addition, previous research has indicated that plumbagin reversibly decreased NADH dehydrogenase activity and blocked respiration in *E. coli*, which was consistent with the proteomic analysis in this study (Imlay and Fridovich, 1992). ATP synthase subunit is an ATP synthase that produces ATP from ADP under the condition of the transmembrane proton gradient. After CUM treatment, the ATP synthase subunit delta protein abundance was significantly down-regulated. NADH dehydrogenase, succinate dehydrogenase, cytochrome reductase and cytochrome oxidase play a considerable role in ETC. In this work, cytochrome oxidase, which was significantly down-regulated at the protein level, could convert molecular oxygen into water and produce vast amounts of ATP molecules. Inhibition of cytochrome oxidase showed the loss of ATP for energy metabolism. Moreover, F0F1-ATP synthase can further utilize the proton gradient generated by ETC to produce ATP (Li et al., 2019), the protein abundances of its subunits B and epsilon were markedly decreased, whereas subunit gamma was different. As a result, the oxidative phosphorylation pathway was restrained, in which the capacities of electron transport in the respiratory chain and ATP synthesis were reduced. Ultimately, the cell respiration was attenuated, as well as the metabolism of organic matter was impacted.

4.3. Amino acid biosynthesis and metabolism

Amino acids are the building blocks of proteins and can be synthesized by microorganisms. Therefore, the biosynthetic and metabolic pathways of amino acids are important for the survival of microorganisms (Zhang et al., 2014). The regulation of biosynthesis can not only effectively prevent bacteria from wasting energy to produce metabolites, but also effectively prevent the transport of metabolites required for survival to the outside of cells. This regulation is essential for the biosynthesis of amino acids, which are indispensable for any enzyme (Kulis-Horn et al., 2014).

Glycine, serine and threonine belong to aliphatic amino acids with similar metabolic pathways. Reversible cleavage/condensation of 2-

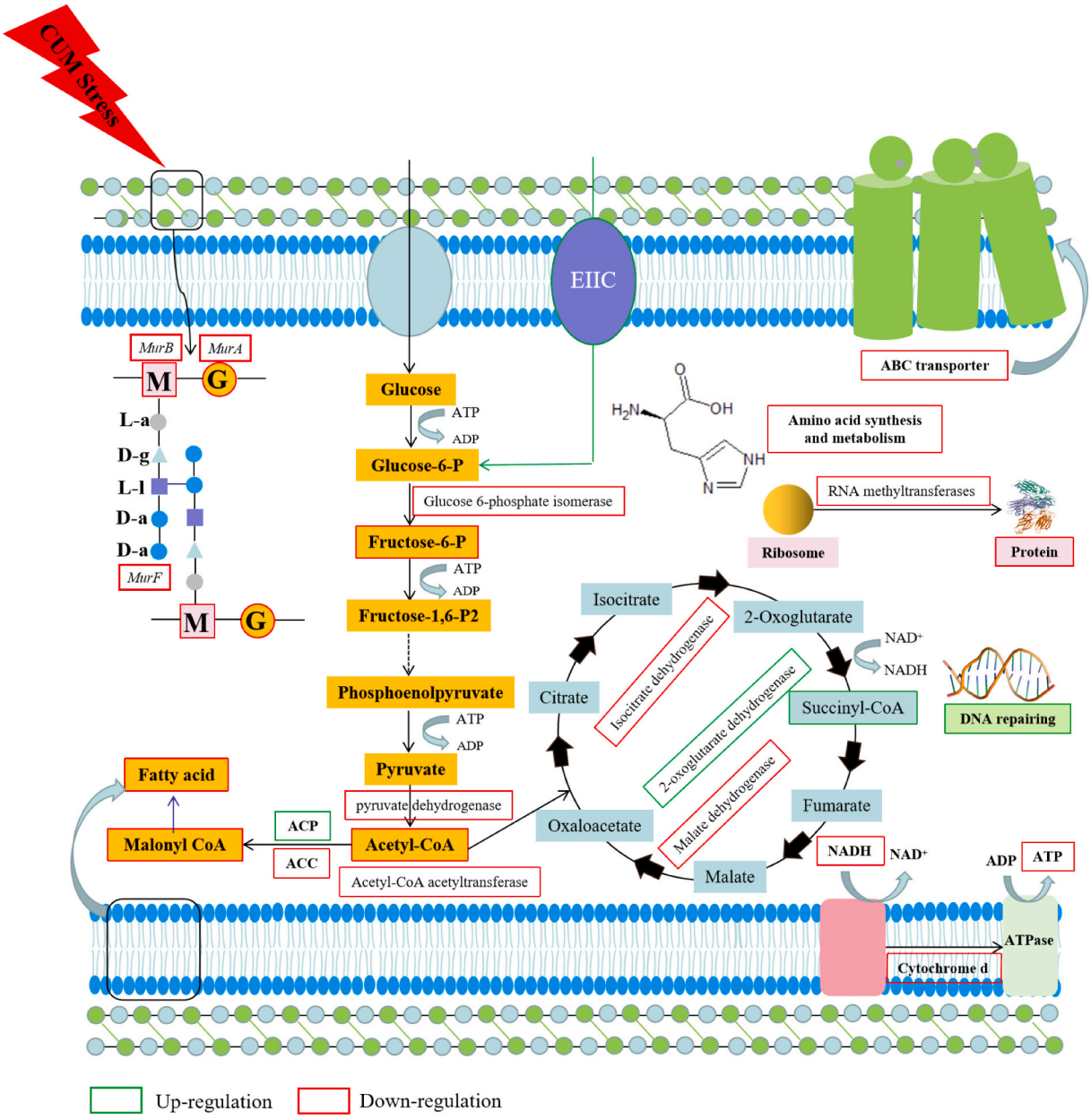

Fig. 5. The proposed cuminaldehyde (CUM) stress response mechanism model of *S. aureus*.

amino-3-ketobutyrate with glycine plus acetyl-CoA are catalyzed by 2-amino-3-ketobutyrate CoA ligase, which is the second reaction of threonine into glycine in the threonine dehydrogenase initiation pathway. Glycine cleavage system H-like protein promotes glycine degradation to obtain 5,10-methylene-tetrahy-drofolate, mainly producing serine, thymine and purine (Brown et al., 2014). GlyA is a serine hydroxymethyltransferase that catalyzes the generation of glycine and methylenetetrahydrofolate from serine and tetrahydrofolate (Tramonti et al., 2018). Noticeable reduction in protein abundances related to glycine, serine and threonine demonstrated that their metabolism was disturbed (Table 2). Methionine and cysteine are two sulfur-containing amino acids required for the bacterial synthesis of protein and glutathione (GSH). Interestingly, Cys/Met metabolism PLP-dependent enzyme associated with cysteine and methionine metabolism, was significantly up-regulated at the protein level. The up-regulation of Cys/Met metabolism PLP-dependent enzyme depleted cysteine and methionine, resulting in the reduction of pathogen growth. In addition, the protein abundance of transaminase was reduced significantly. Transaminase plays a pivotal role in the synthesis of amino acids. It utilizes pyridoxal-5′-phosphate (PLP) as a cofactor to shift the amine group from the amine donor to the ketone or aldehyde acceptor, catalyzing the asymmetric synthesis of chiral amines (Jin et al., 2022). These results indicated that CUM-treated *S. aureus* resulted in the decrease of cysteine and methionine content in cells and the destruction of bacterial growth. Notably, the isoleucine and valine are synthesized by the same enzyme, while leucine, unlike isoleucine and valine, is synthesized by a precursor of L-valine (α-ketoisopentate). As shown in Table 2, the mRNA and protein abundance of 2-isopropylmalate synthase with its encoding gene *leuA* were noticeably decreased. It catalyzes the condensation reaction of 2-keto-3-methylbutanate with acetyl-CoA to generate the intermediate (*S*)-2-isopropylmalate, and produces acetyl coenzyme. The branched-chain alpha-keto acid dehydrogenase E1 component catalyzes the decarboxylation of branched-chain α-keto acids resulting from the transamination of branched-chain amino acids (valine, leucine, and isoleucine). However, *ilvE* which encodes branched-chain aminotransferase for the last procedure of branched-chain amino acids biosynthesis

was significantly down-regulated by 0.66 log2(FC) at the protein level. Interestingly, branched-chain amino acids biosynthesis enzymes have been considered targets for drug development, as these enzymes are momentous in bacteria but not in mammals (Liang et al., 2021). The biosynthesis of branched-chain amino acids associated with the metabolism of carbon, nitrogen and sulfur, was a crossroad of bacterial metabolism (Lobel et al., 2012). In addition, branched-chain amino acids can further form branched-chain fatty acids, which are related to cell membrane formation (Kaneda, 1991). Alternations in the expression of these genes and proteins disrupted amino acid synthesis and metabolic pathways, resulting in more severe damage to the affected cells. Thus, CUM treatment interfered with the amino acid synthesis and metabolism of *S. aureus*, and protein levels, thereby reducing bacterial viability.

4.4. Protein biosynthesis and DNA repair

In general, bacteria need to expend about 50 % of energy to synthesize proteins, of which 20–40 % are associated with ribosomes and other translation factors (Zhang et al., 2020). The synthesis of ribosomal components is a major component of the majority of transcription activities and protein translations. RNA methyltransferases (MTases) was involved in bacterial ribosome biogenesis and regulation (Sunita et al., 2007). Ribosomal RNA small subunit methyltransferase E (RsmE) is responsible for the methylation of U1498 in 16S ribosomal RNA and may play a vital role in the communication between ribosomal subunits (Zhang et al., 2012). After CUM treatment, the RsmE was obviously down-regulated at the protein level, indicating that CUM induced 16S rRNA methylation and disrupted ribosome biogenesis. Bacterial ribosomes are composed of small 30S subunit and large 50S subunit. Ribosomal protein L25 can bind to 5S RNA in the ribosome, forming part of the central bulge. The termination of bacterial protein synthesis is inseparable from the participation of peptide chain releasing factors RF-1 and RF-2, and another factor RF-3 is used to activate them. The proteins expression of 50S ribosomal proteins L25 and RF-3 were dramatically down-regulated under CUM stress, indicating that the self-assembly capacity of the 50S ribosomal subunit was reduced, and the termination of protein synthesis was interfered with, which ultimately led to the reduction of protein synthesis (Kang et al., 2021). Folate, the active form of tetrahydrofolate, is essential for nucleotide biosynthesis, DNA, and RNA (Champier et al., 2012). Because bacteria cannot use exogenous folate derivatives, they must synthesize folic acid from scratch. Hence, dihydrofolate synthase was obviously down-regulated at the protein level under CUN stress, demonstrating CUM might restrain folate biosynthesis and interfere with the synthesis of DNA and protein, resulting in cell death.

To alleviate the adverse effects of DNA damage, cells would initiate various mechanisms for repair (Yang et al., 2017). Proteins involved in DNA replication and repair, including DNA replication protein DnaC and DnaD, recombination and DNA strand exchange inhibitor protein, and single-stranded DNA-binding protein, were significantly up-regulated after CUM stress. Among them, the concentration of single-stranded DNA-binding protein (SSB, 1.71 log2(FC)) was increased after CUM treatment. SSB plays a significant role in DNA replication, safeguarding single-stranded DNA by interacting with various proteins related to DNA replication, recombination and repair. For instance, SSB can combine with single-stranded DNA to avoid producing secondary structures and degrading single-stranded DNA. This up-regulation might help bacteria repair damaged DNA and control protein quality (Michele et al., 2012; Zhou et al., 2011). DNA polymerase III alpha subunit was decreased (−1.86 log2(FC)) after CUM treatment. DNA polymerase III catalyzes the elongation of DNA chains in the process of DNA replication. Its major function is to be responsible for the replication of chromosomal DNA, whereas others are not only participated in DNA repair but also in translesion DNA synthesis (Maki and Furukohri, 2004). The overall activity of DNA repair was up-regulated despite the decline in DNA polymerase III. Hence, up-regulation of proteins related to DNA repair and replication was likely an adaptive strategy for *S. aureus* to cope with CUM stress.

4.5. ABC transporters

ABC transporters, also known as ATP-binding cassettes (ABC), constitute the most prominent family of transmembrane transporters and are omnipresent in all organisms. In bacteria, ABC transporters can transport a variety of substrates such as monosaccharides, oligosaccharides, inorganic ions, amino acids, siderophores, metals, and vitamins, mainly involved in the absorption of nutrients, the output of bacterial toxins and harmful substances (Hu et al., 2017). Oligopeptide permease (Opp) includes two homologous integral membrane proteins OppB and OppC, two homologous nucleotide-binding domains proteins OppD and OppF, and a receptor or substrate-binding protein oppA (Tian et al., 2020). The down-regulation of protein OppB and the up-regulation of proteins OppD and OppF indicated that the protein transport of *S. aureus* was affected by CUM. The gene for iron uptake, *fhuC*, was down-regulated both at transcript and protein levels. Iron is essential for many critical biological processes within bacteria that affect oxygen transport, DNA biosynthesis, energy production, and regulation of gene expression (Lechowicz and Krawczyk-Balska, 2015). Betaine is considered the most reactive natural osmotic protective molecule of bacteria, but its synthesis and accumulation would not occur in cells (Angelidis and Smith, 2003). In the results, *opuCC*, which encodes the substrate-binding region of the ABC-type glycine betaine transport system was significantly down-regulated at the protein level under the stress of CUM, suggesting that the *S. aureus* responded to the osmotic imbalance stress. Proteins related to the cell membrane were reduced obviously after CUM treatment, including ABC transporter permeases (0.34–0.73 log2(FC)), indicating that the cell membrane was destroyed. In addition, the low level of ABC transporters family proteins stated that it was difficult to obtain the amino acids and inorganic ions required to keep osmotic pressure, which might be associated with the damage to the *S. aureus* cell membrane. Consequently, the present findings suggested that CUM could interfere with the transport system and severely damage the *S. aureus* membrane.

5. Conclusion

The study combined transcriptome and proteome data for the first time to gain an insight into the antibacterial mechanism of CUM exposure at the concentration of 0.4 μL/mL to *S. aureus* on sauced beef. Its antibacterial mechanism was mainly attributed to cell envelope damage (decreased peptidoglycan and fatty acids synthesis), energy metabolism disorder (glycolysis, TCA cycle and ETC repression) and amino acids limitation (decreased contents of glycine, serine, threonine, methionine, cysteine and branched-chain amino acids). For survival, *S. aureus* responded to the stress of CUM by activating DNA repair-related genes and proteins. Thus, this study contributes to further understanding of the antimicrobial molecular mechanism of CUM and provides a helpful strategy for the application of CUM in food.

Supplementary data to this article can be found online at https://doi.org/10.1016/j.ijfoodmicro.2022.109930.

Declaration of competing interest

The authors declare no conflict of interest.

Data availability

Data will be made available on request.

Acknowledgments

This work was supported by the R&D Projects in Key Areas of Guangdong Province (No. 2019B020212003) and the R&D Projects in Key Areas of Guangzhou city (No. 202206010177). We thank Guangzhou Gene Denovo Biotechnology Co., Ltd., China, for technical assistance.

References

Alhaji Isa, M., Majumdar, R.S., Haider, S., Kandasamy, S., 2018. Molecular modelling and dynamic simulation of UDP-N-acetylglucosamine 1-carboxyvinyltransferase (MurA) from mycobacterium tuberculosis using in silico approach. Inf. Med. Unlocked 12, 56–66. https://doi.org/10.1016/j.imu.2018.06.007.

Amera, G.M., Khan, R.J., Pathak, A., Jha, R.K., Jain, M., Muthukumaran, J., Singh, A.K., 2020. Structure based drug designing and discovery of promising lead molecules against UDP-N-acetylenolpyruvoylglucosamine reductase (MurB): a potential drug target in multi-drug resistant Acinetobacter baumannii. J. Mol. Graph. S Model. 100, 107675 https://doi.org/10.1016/j.jmgm.2020.107675.

An, H., Douillard, F.P., Wang, G., Zhai, Z., Yang, J., Song, S., Cui, J., Ren, F., Luo, Y., Zhang, B., Hao, Y., 2014. Integrated transcriptomic and proteomic analysis of the bile stress response in a centenarian-originated probiotic bifidobacterium longum BBMN68. Mol. Cell. Proteomics 13 (10), 2558–2572. https://doi.org/10.1074/mcp.M114.039156.

Angelidis, A.S., Smith, G.M., 2003. Three transporters mediate uptake of glycine betaine and carnitine by listeria monocytogenes in response to hyperosmotic stress. Appl. Environ. Microbiol. 69 (2), 1013–1022. https://doi.org/10.1128/AEM.69.2.1013-1022.2003.

Bennett, S.D., Walsh, K.A., Gould, L.H., 2013. Foodborne disease outbreaks caused by Bacillus cereus, Clostridium perfringens, and Staphylococcus aureus-United States, 1998–2008. Clin. Infect. Dis. 57 (3), 425–433. https://doi.org/10.1093/cid/cit244.

Brown, M.J., Russo, B.C., O'Dee, D.M., Schmitt, D.M., Nau, G.J., 2014. The contribution of the glycine cleavage system to the pathogenesis of francisella tularensis. Microbes Infect. 16 (4), 300–309. https://doi.org/10.1016/j.micinf.2013.12.003.

Cao, Y., Jin, X., Levin, E.J., Huang, H., Zong, Y., Quick, M., Weng, J., Pan, Y., Love, J., Punta, M., Rost, B., Hendrickson, W.A., Javitch, J.A., Rajashankar, K.R., Zhou, M., 2011. Crystal structure of a phosphorylation-coupled saccharide transporter. Nature 473 (7345), 50–U58. https://doi.org/10.1038/nature09939.

Cao, Y., Zhou, A., Zhou, D., Xiao, X., Yu, Y., Li, X., 2020. Cronobacter sakazakii CICC 21544 responds to the combination of carvacrol and citral by regulating proton motive force. LWT Food Sci. Technol. 122 https://doi.org/10.1016/j.lwt.2020.109040.

Champier, J., Claustrat, F., Nazaret, N., Montange, M.F., Claustrat, B., 2012. Folate depletion changes gene expression of fatty acid metabolism, DNA synthesis, and circadian cycle in male mice. Nutr. Res. 32 (2), 124–132. https://doi.org/10.1016/j.nutres.2011.12.012.

Chueca, B., Perez-Saez, E., Pagan, R., Garcia-Gonzalo, D., 2017. Global transcriptional response of Escherichia coli MG1655 cells exposed to the oxygenated monoterpenes citral and carvacrol. Int. J. Food Microbiol. 257, 49–57. https://doi.org/10.1016/j.ijfoodmicro.2017.06.002.

Das, S., Singh, V.K., Dwivedy, A.K., Chaudhari, A.K., Deepika, Dubey, N.K., 2021. Nanostructured Pimpinella anisum essential oil as novel green food preservative against fungal infestation, aflatoxin B-1 contamination and deterioration of nutritional qualities. Food Chem. 344. https://doi.org/10.1016/j.foodchem.2020.128574.

Dubin, G., 2002. Extracellular proteases of staphylococcus spp. Biol. Chem. 383 (7–8), 1075–1086. https://doi.org/10.1515/bc.2002.116.

Dupre, J.M., Johnson, W.L., Ulanov, A.V., Li, Z., Wilkinson, B.J., Gustafson, J.E., 2019. Transcriptional profiling and metabolomic analysis of Staphylococcus aureus grown on autoclaved chicken breast. Food Microbiol. 82, 46–52. https://doi.org/10.1016/j.fm.2019.01.004.

European Food Safety, A., European Food Safety, A., European Ctr Dis, P., Co, 2017. The European Union summary report on trends and sources of zoonoses, zoonotic agents and food-borne outbreaks in 2016. EFSA J. 15 (12) https://doi.org/10.2903/j.efsa.2017.5077.

Gao, Y., Liu, Y., Ma, F., Sun, M., Mu, G., Tuo, Y., 2020. Global transcriptomic and proteomics analysis of lactobacillus plantarum Y44 response to 2,2-azobis(2-methylpropionamidine) dihydrochloride (AAPH) stress. J. Proteome 226, 103903. https://doi.org/10.1016/j.jprot.2020.103903.

Ghosh, A., Ricke, S.C., Almeida, G., Gibson, K.E., 2016. Combined application of essential oil compounds and bacteriophage to inhibit growth of Staphylococcus aureus in vitro. Curr. Microbiol. 72 (4), 426–435. https://doi.org/10.1007/s00284-015-0968-6.

Halsey, C.R., Lei, S., Wax, J.K., Lehman, M.K., Nuxoll, A.S., Steinke, L., Sadykov, M., Powers, R., Fey, P.D., 2017. Amino acid catabolism in Staphylococcus aureus and the function of carbon catabolite repression. MBio 8 (1). https://doi.org/10.1128/mBio.01434-16.

Hennekinne, J.-A., De Buyser, M.-L., Dragacci, S., 2012. Staphylococcus aureus and its food poisoning toxins: characterization and outbreak investigation. FEMS Microbiol. Rev. 36 (4), 815–836. https://doi.org/10.1111/j.1574-6976.2011.00311.x.

Hu, S., Yu, Y., Wu, X., Xia, X., Xiao, X., Wu, H., 2017. Comparative proteomic analysis of cronobacter sakazakii by iTRAQ provides insights into response to desiccation. Food Res. Int. 100 (pt.1), 631–639. https://doi.org/10.1016/j.foodres.2017.06.051.

Imlay, J., Fridovich, I., 1992. Exogenous quinones directly inhibit the respiratory NADH dehydrogenase in Escherichia coli. Arch. Biochem. Biophys. 296 (1), 337–346. https://doi.org/10.1016/0003-9861(92)90581-g.

Jin, L.Q., Shentu, J.K., Liu, H.L., Shao, T.C., Liu, Z.Q., Xue, Y.P., Zheng, Y.G., 2022. Enhanced catalytic activity of recombinant transaminase by molecular modification to improve L-phosphinothricin production. J. Biotechnol. 343, 7–14. https://doi.org/10.1016/j.jbiotec.2021.11.002.

Kaneda, T., 1991. Iso- and anteiso-fatty acids in bacteria: biosynthesis, function, and taxonomic significance. Microbiol. Rev. 55 (2), 288. https://doi.org/10.1128/MR.55.2.288-302.1991.

Kang, S., Shi, C., Chang, J., Kong, F., Li, M., Guan, B., Zhang, Z., Shi, X., Zhao, H., Peng, Y., Zheng, Y., Yue, X., 2021. Label free-based proteomic analysis of the food spoiler Pseudomonas fluorescens response to lactobionic acid by SWATH-MS. Food Control 123. https://doi.org/10.1016/j.foodcont.2020.107834.

Kulis-Horn, R.K., Persicke, M., Kalinowski, J., 2014. Histidine biosynthesis, its regulation and biotechnological application in corynebacterium glutamicum. Microb. Biotechnol. 7 (1), 5–25. https://doi.org/10.1111/1751-7915.12055.

Kumar, D., Bansal, G., Narang, A., Basak, T., Abbas, T., Dash, D., 2016. Integrating transcriptome and proteome profiling: strategies and applications. Proteomics 16 (19), 2533–2544. https://doi.org/10.1002/pmic.201600140.

Lechowicz, J., Krawczyk-Balska, A., 2015. An update on the transport and metabolism of iron in listeria monocytogenes: the role of proteins involved in pathogenicity. Biometals 28 (4), 587–603. https://doi.org/10.1007/s10534-015-9849-5.

Li, R., Miao, Y., Yuan, S., Li, Y., Wu, Z., Weng, P., 2019. Integrated transcriptomic and proteomic analysis of the ethanol stress response in Saccharomyces cerevisiae Sc131. J. Proteome 203. https://doi.org/10.1016/j.jprot.2019.103377.

Li, H., Huang, Y., Addo, K.A., Yu, Y., Xiao, X., 2022a. Effects of cuminaldehyde on toxins production of Staphylococcus aureus and its application in sauced beef. Food Control 137. https://doi.org/10.1016/j.foodcont.2022.108960.

Li, H., Zhang, M., Addo, K.A., Yu, Y., Xiao, X., 2022b. Action mode of cuminaldehyde against Staphylococcus aureus and its application in sauced beef. LWT Food Sci. Technol. 155 https://doi.org/10.1016/j.lwt.2021.112924.

Liang, Y.F., Long, Z.X., Zhang, Y.J., Luo, C.Y., Yan, L.T., Gao, W.Y., Li, H., 2021. The chemical mechanisms of the enzymes in the branched-chain amino acids biosynthetic pathway and their applications. Biochimie 184, 72–87. https://doi.org/10.1016/j.biochi.2021.02.008.

Liang, S., Hu, X., Wang, R., Fang, M., Yu, Y., Xiao, X., 2022. The combination of thymol and cinnamaldehyde reduces the survival and virulence of listeria monocytogenes on autoclaved chicken breast. J. Appl. Microbiol. 132 (5), 3937–3950. https://doi.org/10.1111/jam.15496.

Lobel, L., Sigal, N., Borovok, I., Ruppin, E., Herskovits, A.A., 2012. Integrative genomic analysis identifies isoleucine and CodY as regulators of listeria monocytogenes virulence. PLoS Genet. 8 (9), e1002887 https://doi.org/10.1371/journal.pgen.1002887.

Lv, L.X., Yan, R., Shi, H.Y., Shi, D., Fang, D.Q., Jiang, H.Y., Wu, W.R., Guo, F.F., Jiang, X.W., Gu, S.L., Chen, Y.B., Yao, J., Li, L.J., 2017. Integrated transcriptomic and proteomic analysis of the bile stress response in probiotic lactobacillus salivarius LI01. J. Proteome 150, 216–229. https://doi.org/10.1016/j.jprot.2016.08.021.

Maki, H., Furukohri, A., 2004. In: DNA Polymerase III, Bacterial. Encyclopedia of Biological Chemistry, pp. 92–95. https://doi.org/10.1016/B978-0-12-378630-2.00310-8.

Michele, C., Evangelos, S., Hingorani, M.M., Marx, A.D., Jung, C.P., Rothwell, P.J., Seidel, C., Peter, F., 2012. Single-molecule multiparameter fluorescence spectroscopy reveals directional MutS binding to mismatched bases in DNA. Nucleic Acids Res. 40 (12), 5448. https://doi.org/10.1016/j.jprot.2016.08.021.

Monteiro-Neto, V., de Souza, C.D., Gonzaga, L.F., da Silveira, B.C., Sousa, N.C.F., Pontes, J.P., Santos, D.M., Martins, W.C., Pessoa, J.F.V., Carvalho Junior, A.R., Almeida, V.S.S., de Oliveira, N.M.T., de Araujo, T.S., Maria-Ferreira, D., Mendes, S.J.F., Ferro, T.A.F., Fernandes, E.S., 2020. Cuminaldehyde potentiates the antimicrobial actions of ciprofloxacin against Staphylococcus aureus and Escherichia coli. PLoS ONE 15 (5). https://doi.org/10.1371/journal.pone.0232987.

Nie, L., Wu, G., Culley, D.E., Scholten, J.C.M., Zhang, W., 2007. Integrative analysis of transcriptomic and proteomic data: challenges, solutions and applications. Crit. Rev. Biotechnol. 27 (2), 63–75. https://doi.org/10.1080/07388550701334212.

Ostash, B., Walker, S., 2010. Moenomycin family antibiotics: chemical synthesis, biosynthesis, and biological activity. Nat. Prod. Rep. 27 (11), 1594–1617. https://doi.org/10.1039/c001461n.

Poopandi, S., Sundaraj, R., Rajmichael, R., Thangaraj, S., Dhamodharan, P., Biswal, J., Malaisamy, V., Jeyaraj Pandian, C., Jeyaraman, J., 2021. Computational screening of potential inhibitors targeting MurF of brugia malayi wolbachia through multi-scale molecular docking, molecular dynamics and MM-GBSA analysis. Mol. Biochem. Parasitol. 246, 111427 https://doi.org/10.1016/j.molbiopara.2021.111427.

Sunita, S., Purta, E., Durawa, M., Tkaczuk, K.L., Swaathi, J., Bujnicki, J.M., Sivaraman, J., 2007. Functional specialization of domains tandemly duplicated within 16S rRNA methyltransferase RsmC. Nucleic Acids Res. 35 (13), 4264–4274. https://doi.org/10.1093/nar/gkm411.

Suo, Y., Gao, S., Baranzoni, G.M., Xie, Y., Liu, Y., 2018. Comparative transcriptome RNA-seq analysis of listeria monocytogenes with sodium lactate adaptation. Food Control 91, 193–201. https://doi.org/10.1016/j.foodcont.2018.03.044.

Tian, X., Liu, Y., Yu, Q., Shao, L., Li, X., Dai, R., 2020. Label free-based proteomic analysis of Escherichia coli O157:H7 subjected to ohmic heating. Food Res. Int. 128, 108815 https://doi.org/10.1016/j.foodres.2019.108815.

Tramonti, A., Paiardini, A., Paone, A., Bouzidi, A., Giardina, G., Guiducci, G., Magnifico, M.C., Rinaldo, S., McDermott, L., Menendez, J.A., Contestabile, R., Cutruzzola, F., 2018. Differential inhibitory effect of a pyrazolopyran compound on

human serine hydroxymethyltransferase-amino acid complexes. Arch. Biochem. Biophys. 653, 71–79. https://doi.org/10.1016/j.abb.2018.07.001.

Vogel, C., Marcotte, E.M., 2012. Insights into the regulation of protein abundance from proteomic and transcriptomic analyses. Nat. Rev. Genet. 13 (4), 227–232. https://doi.org/10.1038/nrg3185.

Wei, L., Yang, M., Huang, L., Li, J.L., 2019. Antibacterial and antioxidant flavonoid derivatives from the fruits of Metaplexis japonica. Food Chem. 289, 308–312. https://doi.org/10.1016/j.foodchem.2019.03.070.

Xu, D., Wei, M., Peng, S., Mo, H., Huang, L., Yao, L., Hu, L., 2021. Cuminaldehyde in cumin essential oils prevents the growth and aflatoxin B1 biosynthesis of aspergillus flavus in peanuts. Food Control 125. https://doi.org/10.1016/j.foodcont.2021.107985.

Yang, S., Liu, L., Li, D., Xia, H., Su, X., Peng, L., Pan, S., 2016. Use of active extracts of poplar buds against penicillium italicum and possible modes of action. Food Chem. 196, 610–618. https://doi.org/10.1016/j.foodchem.2015.09.101.

Yang, Y., Wang, P., Cui, Y., Wang, Y., 2017. Chemical analysis of DNA damage. Anal. Chem. 90 (1) https://doi.org/10.1021/acs.analchem.7b04247.

Zhang, H., Wan, H., Gao, Z.Q., Wei, Y., Wang, W.J., Liu, G.F., Shtykova, E.V., Xu, J.H., Dong, Y.H., 2012. Insights into the catalytic mechanism of 16S rRNA methyltransferase RsmE (m(3)U1498) from crystal and solution structures. J. Mol. Biol. 423 (4), 576–589. https://doi.org/10.1016/j.jmb.2012.08.016.

Zhang, H., Ma, H., Xie, X., Ji, J., Dong, Y., Du, Y., Tang, W., Zheng, X., Wang, P., Zhang, Z., 2014. Comparative proteomic analyses reveal that the regulators of G-protein signaling proteins regulate amino acid metabolism of the rice blast fungus magnaporthe oryzae. Proteomics 14 (21–22), 2508–2522. https://doi.org/10.1002/pmic.201400173.

Zhang, H., Ge, X., Liu, B., Teng, T., Zhou, Q., Sun, C., Song, C., Liu, B., 2020. Comparative transcriptomic and proteomic analysis of the antibacterial activity of emodin on Aeromonas hydrophila. Aquaculture 529. https://doi.org/10.1016/j.aquaculture.2020.735589.

Zhao, N., Jiao, L., Xu, J., Zhang, J., Qi, Y., Qiu, M., Wei, X., Fan, M., 2022. Integrated transcriptomic and proteomic analysis reveals the response mechanisms of alicyclobacillus acidoterrestris to heat stress. Food Res. Int. 151, 110859 https://doi.org/10.1016/j.foodres.2021.110859.

Zheng, S., Jing, G., Wang, X., Ouyang, Q., Jia, L., Tao, N., 2015. Citral exerts its antifungal activity against penicillium digitatum by affecting the mitochondrial morphology and function. Food Chem. 178, 76–81. https://doi.org/10.1016/j.foodchem.2015.01.077.

Zhou, R., Kozlov, A., Roy, R., Zhang, J., Korolev, S., Lohman, T., Ha, T., 2011. SSB functions as a sliding platform that migrates on DNA via reptation. Cell 146 (2), 222–232. https://doi.org/10.1016/j.cell.2011.06.036.